HHS Public Access

Author manuscript

Diabetes. Author manuscript; available in PMC 2025 September 09.

SIRT6 Is a Key Regulator of Pancreatic β-cell Survival and Function During Aging

Jimin Park[1,#], **Sandali D. Lokuge**[2,#], **Menghao Huang**[1,3,4,#], **Shen Wang**[1,#], **Sheng Liu**[4,5,6], **Jingru Liang**[1], **Ramkumar Katturajan**[1], **Corinn Marakovits**[1], **Zhihong Yang**[7], **Jun Wan**[2,4,5,6], **X. Charlie Dong**[1,2,3,5,6,*]

[1]Department of Biochemistry and Molecular Biology, School of Medicine, Indiana University, Indianapolis, IN, USA.

[2]Luddy School of Informatics, Computing, and Engineering, Indiana University Indianapolis, Indianapolis, IN, USA.

[3]Center for Diabetes and Metabolic Diseases, Indiana University School of Medicine, Indianapolis, IN, USA.

[4]Melvin & Bren Simon Comprehensive Cancer Center, Indiana University School of Medicine, Indianapolis, IN, USA

[5]Department of Medical and Molecular Genetics, Indiana University School of Medicine, Indianapolis, IN, USA.

[6]Center for Computational Biology and Bioinformatics, Indiana University School of Medicine, Indianapolis, IN, USA

[7]Department of Medicine, Division of Gastroenterology and Hepatology, Indiana University School of Medicine, Indianapolis, IN, USA.

Abstract

Pancreatic β cells undergo senescence and death during aging; however, the underlying mechanisms remain incompletely understood. The aims of this study were to investigate the role of sirtuin 6 (SIRT6) in the regulation of β-cell survival and function during aging. Pancreatic β-cell-specific *SIRT6* transgenic mice (TgSIRT6) were generated for the study. DNA damage, cell death, and cell proliferation were analyzed by immunofluorescence microscopy. Gene expression was analyzed by RNA-seq. Candidate genes and pathways were validated in the INS-1 cell line. SIRT6 protein levels were decreased in pancreatic β cells during aging. TgSIRT6 mice exhibited less DNA damage and cell death including apoptosis, necroptosis, and pyroptosis in β cells

[*]**Corresponding author**: Department of Biochemistry and Molecular Biology, School of Medicine, Indiana University, Indianapolis, IN 46202, USA. xcdong@iu.edu.

Guarantor's statement: Dr. Charlie Dong is the guarantor of this work and he had full access to all the data in the study and takes responsibility for the integrity of the data and the accuracy of the data analysis.

Author contributions: JP performed experiments and wrote manuscript; MH performed experiments; SW analyzed transcriptomic data and interpretation; SDL analyzed transcriptomic data; JL contributed to the animal model development; RK analyzed transcriptomic data; CM interpreted data; JW performed data analysis and interpretation; XCD performed experimental design, data analysis, and wrote the manuscript.

[#]These authors contributed equally.

Conflict of interest statement: None.

than that in wildtype mice. TgSIRT6 mice had increased number of large islets and an increase in total islet area in pancreas compared to wildtype mice. As a result, TgSIRT6 mice showed better glucose tolerance and glucose-stimulated insulin secretion than wildtype mice. RRAD and GEM like GTPase 2 (REM2), an endogenous inhibitor of high-voltage-activated calcium channels, was negatively regulated by SIRT6. Knockdown of *Rem2* in INS-1 cells partially rescued the SIRT6 deficiency- and palmitic acids-induced DNA damage, lipid peroxidation, and cell death. *Rem2* β-cell-specific knockout mice had less DNA damage and cell death in β cells than that in wildtype mice. Our data suggest that SIRT6 is a critical anti-aging factor in pancreatic β cells. SIRT6 overexpression significantly reduces DNA damage and cell death. Thus, SIRT6 can be a therapeutic target for reversing β-cell aging.

Keywords

Aging; apoptosis; beta cell; necroptosis; pyroptosis; REM2; SIRT6

Introduction

Aging is a major biological driver of metabolic dysfunction, including impaired pancreatic β-cell function, which is crucial for maintaining glucose homeostasis (1–3). As individuals age, the prevalence of metabolic disorders, such as type 2 diabetes (T2D), rises significantly, reaching higher than 20% among those aged 65 and older (3). Despite the clear link between aging and T2D, the molecular mechanisms underlying β-cell dysfunction during aging remain poorly understood.

Pancreatic β cells, responsible for insulin secretion, undergo a decline in both mass and function with age (4–6). This decline is exacerbated by oxidative stress, DNA damage, and cell death, which contribute to reduced insulin secretion and impaired glucose metabolism (1, 3, 7–10). Understanding the molecular mechanisms of β-cell aging is therefore crucial, not only for addressing diabetes but also for mitigating broader metabolic dysfunction associated with aging.

Sirtuin 6 (SIRT6), a member of the NAD^+-dependent deacetylase family, has emerged as a key regulator of aging and metabolic homeostasis (11–13). SIRT6 is involved in maintaining genomic stability, promoting DNA repair, and regulating metabolic homeostasis (11, 14–20). SIRT6 gene expression and enzymatic activity decline with age in pancreatic islets, which parallels with the progression of β-cell dysfunction (10). SIRT6 deficiency in β cells leads to mitochondrial dysfunction, disrupted calcium homeostasis, and impaired glucose-stimulated insulin secretion (GSIS) whereas SIRT6 overexpression has been shown to enhance insulin secretion and reduce palmitic acid-induced β-cell apoptosis (10, 21–24). To further investigate the role of SIRT6 in aging-related β-cell survival and function, we selected RRAD and GEM like GTPase 2 (REM2) as a potential downstream candidate since they both are involved in calcium dynamics and insulin secretion. REM2 has been reported as a potent endogenous inhibitor of high-voltage-activated calcium channels (HVACCs) like $Ca_V1.2$ (encoded by the *CACNA1C* gene) and $Ca_V2.1$ (encoded by the *CACNA1A* gene), which are critical for calcium influx during insulin secretion (25–27). REM2 also inhibits

Ca^{2+}/calmodulin-dependent protein kinase II (CaMKII) in neurons (28). A REM2 gene variant (G96A) is associated with long QT syndrome type 2 severity (29). Under normal conditions, REM2 gene is highly abundant in animal brains compared to other tissues in the body and its expression peaks at postnatal week two in mice (30). The *Rem2* gene in Zebrafish is required for neuronal development as Rem2 morpholino causes impaired mid-brain development and a 3.5-fold increase in the apoptosis/proliferation ratios at 36 hours of embryo development (31). One study has documented that REM2 maintains human embryonic stem cells (hESCs) by suppressing both p53 transcriptional activity and cyclin D1 (32). Another study has reported that REM2 increases endothelial cell proliferation by suppression of human p14(ARF) or mouse p19(ARF) (33). *Rem2* gene can be induced by 25 mM glucose in mouse MIN6 insulinoma cells. Overexpression of *Rem2* in MIN6 cells potently inhibits high glucose-stimulated insulin secretion (26).

In this study, we attempted to address the role of SIRT6 and REM2 in pancreatic β-cell aging using both cell and animal models. To achieve this goal, we developed an inducible SIRT6 transgenic mouse model and *Rem2* β-cell-specific knockout mouse model. We analyzed DNA damage, cell proliferation, and cell death in mouse pancreatic sections and cultured β cells.

Methods

Animals

We have developed a conditional SIRT6 transgenic mouse line by placing a floxed STOP cassette in front of the human *SIRT6* gene coding sequence fused with a 3x HA tag sequence as previously described (34). SIRT6 conditional transgenic mice were crossed with *Ins1-Cre/ERT2* mice obtained from the Jackson Laboratory (strain #: 026802) to generate *SIRT6* β-cell-specific transgenic mice (TgSIRT6). Tamoxifen was administered to both control (including floxed mice and Cre mice) and TgSIRT6 mice via oral gavage at a dosage of 4 mg/mouse in corn oil for four consecutive days. For the 10- and 16-month age groups, tamoxifen was administered when the mice reached 5 and 11 months of age, respectively.

Rem2 β-cell-specific knockout (*Rem2* βKO) mice were generated by crossing *Rem2* floxed mice (kindly provided by Dr. Daniel J. Liput from the Laboratories of Molecular Physiology at the National Institute on Alcohol Abuse and Alcoholism, National Institutes of Health) with *Ins1-Cre/ERT2* mice. The *Rem2* gene knockout was initiated by injecting tamoxifen at 5 months of age and phenotyping was performed at 10 and 16 months of age.

Animals were housed in groups (up to five per cage) with paper bedding and enrichment in vented cages with automated water in a specific pathogen-free facility with controlled temperature (22 ± 2 °C), humidity (60 ± 5%), and a regular 12:12 light/dark cycle. TgSIRT6 transgenic and control WT mice were maintained on a normal chow diet containing 18 kcal% fat (Envigo 2018SX). To add environmental stress to pancreatic β cells, *Rem2* βKO and control mice (including floxed mice and Cre mice) at 5 months of age were treated with a high-fat diet containing 60 kcal% fat (Research Diets # D12492) for 11 weeks and then switched to normal chow until euthanasia. TgSIRT6 transgenic mice and their age-matched control littermates were subjected to the same experimental procedures at the same time.

All animal procedures followed the National Institutes of Health (NIH) Guide for the Care and Use of Laboratory Animals and were approved by the Indiana University School of Medicine Institutional Animal Care and Use Committee. Data were collected from both male and female mice.

Human pancreatic specimens

Formalin-fixed paraffin-embedded human pancreatic specimens were provided by the NIDDK-funded Integrated Islet Distribution Program (IIDP) (RRID:SCR_014387) at City of Hope, NIH grant U24DK098085. Human subject information was described in the Supplementary Table 1.

RNA sequencing and data analysis

Primary pancreatic islets were isolated from 10- and 16-month control and TgSIRT6 mice at the Islet and Physiology Core of the Indiana University Center for Diabetes and Metabolic Diseases as previously described (35). Total RNAs were extracted from the pancreatic islets using an RNeasy Plus Mini Kit (Qiagen). RNA integrity was verified using an Agilent Bioanalyzer and only samples with RNA Integrity Numbers (RIN) above 8 were used. Libraries were prepared using a Stranded mRNA Prep Kit (Illumina) and sequenced on an Illumina NovaSeq 6000 platform. Sequencing quality was assessed using FastQC (v0.12.1). Adapter sequences were removed and low-quality or short reads were filtered using Trim Galore (v0.6.10). The trimmed reads were aligned to the mouse reference genome (GRCm38/M25) using STAR aligner (v.2.7.11a). Reads with low mapping quality (MAPQ < 10) were excluded for further analysis using ngsutils (v0.4.21). Gene-level read counts were quantified using featureCounts (v2.0.0) with GENCODE annotation (vM25). Differential gene expression analysis was performed using the edgeR package (v3.40.2), with significantly differentially expressed genes (DEGs) defined by FDR-adjusted p-values < 0.05 and the magnitude of log2 fold change $|\log_2 FC| > 1$. Gene Ontology (GO) analysis on selected genes and Gene Set Enrichment Analysis (GSEA) on all genes were performed using the ClusterProfiler package (v4.6.2). GO terms, Kyoto Encyclopedia of Genes and Genomes (KEGG) pathways, and Hallmark gene sets with an adjusted p-value less than 0.05 considered to be significantly enriched.

Cell culture and DNA constructs

INS-1 cells (originally from Dr. Christopher Newgard) were cultured in RPMI 1640 medium, supplemented with 2 mM L-glutamine, 1 mM sodium pyruvate, 10 mM HEPES, 0.05 mM β-mercaptoethanol, 100 U/ml penicillin, 100 μg/ml streptomycin, and 10% FBS, and maintained at 37 °C in 5% CO_2, as previously reported (36). The cells had no mycoplasma contamination. Palmitic acids (Millipore Sigma) were conjugated with fatty acid-free BSA and introduced into the culture medium at a final concentration of 0.2 mM, as previously described (10). For DNA constructs, human *SIRT6* and the catalytically inactive *SIRT6* H133Y were cloned into a pcDNA3.1 vector and single guide RNAs (sgRNAs) targeting rat *Sirt6* and *Rem2* were designed using the GPP sgRNA designer tool on the Broad Institute website and cloned into a lentiCRISPR v2 vector (a gift from Dr. Feng Zhang, Addgene plasmid # 52961).

Quantitative PCR

Total RNAs were isolated using TRI Reagent (Millipore Sigma) and cDNA was synthesized using a high-capacity cDNA reverse transcription kit (Thermo Fisher Scientific). Quantitative PCR (qPCR) reactions were performed with the gene primers described in the Supplemental Table 2. Relative gene expression changes were analyzed using the $2^{(-\Delta\Delta Ct)}$ method (37).

Western blot analysis

Protein extracts were prepared in lysis buffer (50 mM HEPES, pH 7.5, 150 mM NaCl, 10% glycerol, 1% Triton X-100, 1.5 mM $MgCl_2$, 1 mM EGTA) supplemented with protease inhibitor cocktail (Millipore Sigma). Protein samples were resolved on an SDS-PAGE gel and transferred to nitrocellulose membrane (Santa Cruz Biotechnology). Membranes were incubated with primary antibodies as described in the Supplemental Table 2. Proteins were detected using HRP-conjugated secondary antibodies, followed by ECL detection reagents (Thermo Fisher Scientific). Protein signals were scanned using a ChemiDoc MP System (Bio-Rad Laboratories). Quantitative analysis was performed using the ImageJ software.

Glucose tolerance test (GTT) and serum insulin assays

GTT and serum insulin analysis were performed one week before animal euthanasia. After a 6-hour fast, mice were injected intraperitoneally with 2 g/kg of D-glucose. Blood glucose levels were measured from tail blood using a Contour glucometer (Ascensia Diabetes Care) at 0, 15, 30, 60, and 120 minutes after glucose injection. Area under the curve (AUC) analysis was performed using GraphPad Prism 10. For blood insulin analysis, blood samples were collected from tail vein at 0 and 15 minutes after glucose injection. Blood samples were centrifuged at 5000 × g for 5 minutes at 4 °C and sera were collected. Serum insulin levels were determined using an Ultra Mouse Insulin ELISA kit (Crystal Chem Inc, #90080), following the manufacturer's instructions.

Histological analysis

Mouse pancreatic tissue specimens were fixed in formalin and processed for paraffin embedding and sectioning at the Indiana University Histology Core. Tissue sections (5 μm thick) were deparaffinized in xylene and rehydrated in a graded ethanol series. Tissue sections were stained with hematoxylin and eosin (H&E). Images were captured using a Leica DM750 microscope with an EC3 digital camera and processed using ImageJ. Islet areas were quantified using ImageJ. Islet boundaries were manually traced for calculating the total islet area in pixels. A total of 100 islets were randomly selected and measured for each group. Islets were divided into small, medium, and large categories according to pixel counts. After dissection, pancreata were weighed, laid flat in cassettes, fixed for 4 h in 4% paraformaldehyde, dehydrated, and embedded in paraffin. Longitudinal pancreatic sections were cut at a 5-μm thickness, collected at 250-μm intervals, and plated on glass slides. This resulted in the collection of 6 sections per pancreas. Sections were immunolabeled with guinea pig anti-insulin and HRP-conjugated donkey anti-guinea pig antibodies (Vector Labs). Insulin immunolabeling was visualized with an IHC kit (Vector Labs), and sections

were counterstained with Eosin-Y (Fisher). All images were acquired on a slide scanner at ×20 magnification.

Immunofluorescence microscopy

Formalin-fixed, paraffin-embedded sections of mouse pancreatic samples (5 μm thick) were processed for deparaffinization and rehydration by sequential incubations in 100% xylene, 50% xylene and 50% ethanol, 100% ethanol, 95% ethanol, 70% ethanol, and 50% ethanol, and rinsing with running tap water. Antigen retrieval was performed in 10 mM sodium citrate buffer for 20 minutes. Tissue sections were blocked with 10% donkey serum for 1 hour at room temperature, followed by three washes with PBS. Immunofluorescence was performed using the primary antibodies described in the Supplemental Table 2 and detected using fluorophore-conjugated secondary antibodies. INS-1 cells grown on glass-bottom dishes were fixed with 4% paraformaldehyde for 10 minutes at room temperature, then washed three times with PBS and incubated overnight with primary antibodies followed by incubation with fluorophore-conjugated secondary antibodies. Images were captured using a Zeiss fluorescence microscope and analyzed using ImageJ.

TUNEL assays

Cell death was analyzed using a TUNEL assay kit (Thermo Fisher # C10617) according to the kit manual. For pancreatic sections, at least 10 fields with at least 8 β-cells per field at ×630 magnification on a Zeiss fluorescence microscope were counted for each specimen. For INS-1 cells, 40 cells were counted for each group at ×200 magnification.

CUT&RUN analysis

To analyze chromatin association events of SIRT6 in INS-1 cells, we prepared cells under normal culture conditions and processed cells for CUT&RUN analysis using a kit (#14–1048) from Epicypher using either control IgG or antibodies for SIRT6, H3K9ac, and H3K4me3. DNA libraries were prepared using a kit (14–1001) from Epicypher. Sequencing was performed on an Illumina NextSeq 2000 system. Adapter sequences and low-quality base calls were trimmed off. The resulting high-quality reads were aligned to the rat reference genome rn6 using bowtie2. Duplicate reads were removed using the Picard program. Peaks were called using the SEACR algorithm.

Statistical analysis

All statistical data were expressed as mean ± SEM. Statistical analysis was performed using Prism 10 software from GraphPad (La Jolla, CA). Comparisons between two groups were performed using a two-tailed unpaired *Student* t-test, and comparisons for more than two groups were performed using a one-way or two-way analysis of variance followed by the Tukey post-hoc test.

Results

SIRT6 gene expression is decreased in pancreatic β cells during aging

To investigate the effect of aging on *SIRT6* gene expression in pancreatic β cells, we performed immunofluorescence microscopy of pancreatic sections from 6, 10, and 16 months old wildtype mice. First, we confirmed pancreatic β-cell aging using a common senescence marker – P16 (CDKN2A). As the antibody detected both P16 and P15 (CDKN2B), P15/16^{+} β cell percentages were significantly increased from 6 months to 10 or 16 months (Fig. 1a,b). Immunofluorescent staining of SIRT6 revealed a significant age-dependent decrease in aged pancreatic β cells (Fig. 1c,d). Similar changes were observed in human β cells in aged non-diabetic human subjects (Fig. 1e–j). These data suggest that SIRT6 may play a role in the regulation of β-cell aging.

SIRT6 overexpression improves β-cell mass and function

To further explore the role of SIRT6 in β-cell aging, we generated β-cell-specific SIRT6 transgenic mice using a tamoxifen-inducible Cre line driven by the endogenous mouse Ins1 gene promoter and a conditional SIRT6 transgene with a floxed STOP cassette as we reported previously (34). Immunofluorescent staining using an HA-Tag antibody confirmed that the SIRT6 transgene was specifically expressed in β cells of TgSIRT6 mice (Fig. 2a and Supplemental Fig.1a, b). It was noted that SIRT6 protein levels were also decreased in β cells of 16-month TgSIRT6 mice compared to 10-month TgSIRT6 mice (Supplemental Fig. 2 a–c). Next, we analyzed pancreatic islets in control and TgSIRT6 mice at ages of 10 and 16 months. Total islet areas were significantly increased in TgSIRT6 mice compared to WT mice at both 10 and 16 months (Fig. 2b, c). β cell mass in TgSIRT6 mice trended up at 10 months and significantly increased at 16 months of age (Fig. 2d). Glucose tolerance tests were performed to assess glucose metabolism in control and TgSIRT6 mice at 10 and 16 months of age. TgSIRT6 mice showed better glucose tolerance than control mice with a significant decrease in AUC at both 10 and 16 months of age (Fig. 2e, f). To further investigate the effect of SIRT6 overexpression on insulin secretion, we performed glucose-stimulated insulin secretion (GSIS) in 16-month-old mice. Serum insulin levels were significantly higher in TgSIRT6 mice than in control mice at 15 minutes after glucose injection (Fig. 2g). These data suggest that SIRT6 overexpression can reverse the decline of β-cell mass, insulin secretion, and glucose tolerance.

SIRT6 overexpression reduces DNA Damage and cell death in β cells during aging

To investigate how SIRT6 overexpression protects β cells during aging, we performed immunofluorescent staining of markers of senescence, DNA damage, cell proliferation, and cell death in control and TgSIRT6 mouse pancreatic sections. P15/16 trended lower at 10 months but significantly decreased in β cells of TgSIRT6 mice at 16 months of age (Supplemental Fig. 3a, b). Similar changes of another senescence marker P21 or cyclin-dependent kinase inhibitor 1A (CDKN1A) were also observed in β cells of TgSIRT6 mice (Supplemental Fig. 4a, b). 53BP1, a DNA damage marker, was significantly elevated in control β cells in 16-month-old mice compared to 10-month-old mice. SIRT6 overexpression reduced DNA damage by approximately 50% (Fig. 3a, b). Ki67, a proliferation marker, was remarkably increased in TgSIRT6 β cells compared to control

β cells at both 10 and 16 months of age (Fig. 3c, d). Next, we analyzed cell death markers. TUNEL staining showed an increase in cell death in control β cells but a significant decrease in TgSIRT6 β cells at both 10 and 16 months of age (Fig. 4a, e). Cleaved caspase 3 (CASP3), an apoptosis marker, was also significantly decreased in TgSIRT6 β cells compared to control β cells at both 10 and 16 months of age (Fig. 4b, f). Gasdermin D (GSDMD), a marker of pyroptosis, was significantly decreased in TgSIRT6 β cells compared to control β cells at both 10 and 16 months of age (Fig. 4c, g). Co-staining of GSDMD and SIRT6 also revealed a general inverse correlation between GSDMD and SIRT6 protein levels but not necessarily down to single-cell levels (Supplemental Fig. 5 a–d). Phosphorylated mixed lineage kinase domain-like pseudokinase (p-MLKL), a marker of necroptosis, was also remarkably decreased in TgSIRT6 β cells compared to control β cells at both 10 and 16 months of age (Fig. 4d, h). These data suggest that SIRT6 overexpression can reduce DNA damage, senescence and multiple forms of cell death and increase proliferation in β cells.

To further investigate the transcript changes at the transcriptomic levels, we performed RNA-seq analysis of primary islets from 10- and 16-month-old control and TgSIRT6 mice. Among DEGs between 10-month and 16-month control mouse islets, 1,979 and 825 genes were upregulated and downregulated, respectively (Supplemental Fig. 6a). In the up DEGs, inflammation, type I diabetes, and cell death related biological processes were highly overrepresented (Supplemental Fig. 6b). In the down DEGs, circadian rhythm, pancreatic β cell proliferation, hormone secretion, and energy homeostasis related processes were significantly enriched (Supplemental Fig. 6c). At 10 months of age, 642 genes were upregulated and 599 genes were downregulated in TgSIRT6 mouse islets compared to control islets (Supplemental Fig. 7a). The pathways of ribosome, pancreatic secretion, oxidative phosphorylation and biological processes such as mitochondrial complexes were enriched in up-regulated genes in the 10-month TgSIRT6 islets (Supplemental Fig. 7b, c). At age of 16 months, more genes tended to be downregulated in TgSIRT6 mouse islets compared to age-matched control islets (Supplemental Fig. 8a), including genes involved in inflammation, oxidative stress, calcium homeostasis, cell death, and others whereas genes associated with vesicle processing and mitochondrial complex I assembly tended to be upregulated (Supplemental Fig. 8b). KEGG and Hallmark pathway analyses also revealed that protein export and autophagy pathways were positively regulated in addition to pancreatic β cell hallmark genes whereas inflammation, cellular senescence, and apoptosis hallmark genes were negatively regulated in the 16-month TgSIRT6 mouse islets (Supplemental Fig. 9a, b). Intriguingly, the number of overlapped genes between TgSIRT6 and control mouse islets at both 10 months and 16 months of age was relatively small, only 18 upregulated and 41 downregulated genes, respectively (Supplemental Fig. 10a, b and Supplemental Table 3).

Interestingly, principal component analysis (PCA) revealed that 16-month TgSIRT6 islet transcriptomes shifted toward 10-month control islet transcriptomes (Supplemental Fig. 11a). Next, we incorporated the comparisons between control and TgSIRT6 islets at both time points (Supplemental Fig. 11 b–e). Most DEGs (1,883) in the 16-month TgSIRT6 islets behaved more like counterparts in the 10-month control islets (Fig. 5a and Supplemental Fig. 11b). The majority (1,265) of upregulated DEGs in the 16-month control islets relative

to 10-month control islets were downregulated in the 16-month TgSIRT6 islets relative to 16-month control islets (Fig. 5b). Among those common DEGs, biological processes and pathways involved in inflammation, type I diabetes, oxidative stress, cell senescence, and cell death were highly represented (Fig. 5c). For example, genes involved in apoptosis, pyroptosis, calcium regulation, necroptosis, ferroptosis, senescence, and DNA damage and repair in the 16-month TgSIRT6 islets had similar expression profiles to the 10-month control islets but not 16-month control islets (Fig. 5 d–f, Supplemental Fig. 12 a–c, and Supplemental Fig. 13). These data suggest that SIRT6 overexpression slows down β-cell aging.

SIRT6 negatively impacts the Rem2 gene expression in β cells

As our RNA-seq data revealed a role of SIRT6 in the regulation of calcium homeostasis in β cells, we next investigated a potential role of the *Rem2* gene, a known inhibitor of voltage-activated Ca^{2+} channels, in β-cell aging. Although REM2 mRNA levels were not significant different between control and TgSIRT6 mouse islets at 16 months of age (Fig. 5f), REM2 protein levels were significantly reduced in β cells of TgSIRT6 mice compared to control mice at both 10 and 16 months of age (Fig. 6a, b). Additionally, REM2 protein levels were also significantly elevated in β cells of aged non-diabetic human subjects compared to young counterparts (Supplemental Fig. 14). To further investigate the regulation of the *Rem2* gene by SIRT6, we transfected INS-1 cells with either a control sgRNA or *Sirt6* sgRNA. SIRT6 knockdown significantly increased REM2 mRNA and protein levels (Fig. 6 c–e). To further confirm whether the catalytic activity of SIRT6 is required or not, we transfected INS-1 cells with either wildtype SIRT6 or a catalytically inactive SIRT6 mutant (SIRT6-H133Y). Indeed, wildtype but not mutant SIRT6 suppressed the *Rem2* gene expression at both mRNA and protein levels (Fig. 6 f–h). To analyze whether SIRT6 is associated the *Rem2* gene promoter region at the chromatin level, we conducted CUT&RUN analysis using three different SIRT6 antibodies. Our data showed that at least two SIRT6 antibodies detected SIRT6 association with the Rem2 gene promoter region as well as histone marker H3K9ac (a substrate of SIRT6 enzyme) (Supplemental Fig. 15), suggesting a potential role of SIRT6 in the regulation of Rem2 chromatin. Approximately 30% of the chromatin association events in the 2,000 bp gene promoters were shared by SIRT6 and H3K9ac datasets (Supplemental Fig. 16a). Among the shared genes, enriched pathways included apoptosis, cell division, DNA damage, insulin secretion, and calcium transport (Supplemental Fig. 16b).

Rem2 knockdown partially rescues the SIRT6-deficiency defects in β cells

To further explore the functional relationship between SIRT6 and REM2, we performed single or double gene knockdowns in INS-1 cells in the absence or presence of palmitic acids. *Sirt6* and *Rem2* gene knockdowns were confirmed by immunostaining (Fig. 6d, e, Supplemental Fig. 17a, b). *Sirt6* knockdown increased DNA damage indicated by 53BP1 staining in INS-1 cells and palmitic acid treatment further exacerbated that whereas *Rem*2 knockdown partially reversed DNA damage (Supplemental Fig. 18a, c). Sirt6 knockdown markedly reduced cell proliferation marker Ki67 but Rem2 knockdown partially reversed the proliferation defect (Supplemental Fig. 18b, d). Next, we analyzed lipid peroxidation, a trigger of ferroptosis. Sirt6 knockdown in INS-1 cells significantly elevated lipid

peroxidation levels indicated by an increase in 4-HNE staining and a decrease in glutathione peroxidase 4 (GPX4), a key enzyme in anti-lipid peroxidation whereas Rem2 knockdown partially reversed lipid peroxidation (Supplemental Fig. 19a, b, h, i). Sirt6 knockdown increased DNA damage indicated by p-H2A.X staining whereas Rem2 knockdown partially reduced that (Supplemental Fig. 19c, j). Sirt6 knockdown increased apoptosis. necroptosis, and pyroptosis in INS-1 cells whereas Rem2 knockdown partially rescued from those forms of cell death (Supplemental Fig. 19d–g, k–n). These data suggest that REM2 mediates a part of the SIRT6-deficiency-induced defects.

Rem2 β-cell-specific knockout mice have improved β-cell survival and function

To investigate the role of REM2 in β cells *in vivo*, we generated *Rem2* β-cell-specific knockout (*Rem2* βKO) mice using a *Rem2* floxed mouse strain and an Ins1-Cre^{ERT2} line. Immunostaining analysis confirmed that REM2 was specifically deficient in pancreatic β cells (Fig. 7a and Supplemental 20a, b). Histological analysis showed an increase in islet area in the *Rem2* βKO mice than that in control mice at both 10 and 16 months of age (Fig. 7b, c). *Rem2* βKO mice had a significant increase in β -cell mass at both 10 and 16 months of age (Fig. 7d). Glucose-stimulated insulin secretion was significantly increased at 15 minutes post-glucose load in *Rem2* βKO mice at both 10 and 16 months of age (Fig. 7e, f). *Rem2* βKO mice had better glucose tolerance than control mice at both 10 and 16 months of age (Fig. 7g, h). Immunostaining analysis revealed that *Rem2* βKO mice had a significant decrease in DNA damage but an increase in proliferation in β cells (Fig. 8a–d). Cell senescence shown by P15/16 and P21 was significantly reduced in β cells of the *Rem2* βKO mice at 16 months of age (Supplemental Figs. 21a, b and 22a, b). Cell death analysis also revealed that *Rem2* gene knockout significantly reduced multiple forms of cell death including apoptosis, pyroptosis, and necroptosis (Fig. 8e–l). These data suggested that REM2 is a negative regulator for β-cell survival and function.

Discussion

SIRT6 has been implicated in animal longevity. *Sirt6* systemic knockout mice die prematurely after birth (11, 38). SIRT6-deficient monkeys also die hours after birth due to severe developmental retardation (13). *Sirt6* transgenic male mice have 13–16% longer lifespan than WT controls (12). Those male transgenic mice have lower serum IGF1 levels. Interestingly, *Ngn3*-Cre-mediated *Sirt6* gene knockout mice have relatively normal β-cell differentiation and proliferation (22). However, β-cell SIRT6 deficiency leads to insulin secretion defect due to mitochondrial dysfunction, oxidative stress, and other factors (22–24). SIRT6-deficient β cells are more susceptible to palmitic acid-induced apoptosis than wildtype β cells (10). In this current study, we have demonstrated that SIRT6 overexpression can significantly reduce multiple forms of cell death including apoptosis, necroptosis, and pyroptosis triggered by age or lipotoxicity. As SIRT6 plays a critical role in DNA repair and genome integrity (11, 18, 39, 40), age-associated SIRT6 decline may contribute to the elevated DNA damage levels in aged β cells. Although SIRT6 has been widely reported for its function in anti-apoptosis (41–46), its role in necroptosis and pyroptosis remains poorly understood. Knockdown of SIRT6 in prostate cancer cell lines increases TNFα-induced necroptosis by activation of RIPK3 and MLKL (47). SIRT6 can inhibit oxidized LDL-induced endothelial cell pyroptosis by deacetylation of apoptosis-associated

speck-like protein (ASC, officially as PYCARD) (48). SIRT6 also inhibits TNFα-induced vascular endothelial cell pyroptosis by suppression of the Lin28b/Let-7 pathway (49).

Calcium flux regulation plays a critical role in insulin secretion from pancreatic β cells (6, 50). SIRT6 has been implicated in the regulation of calcium homeostasis (23, 51). It has been reported that SIRT6 regulates calcium signaling through modulation of intracellular levels of ADP-ribose that can activate transient receptor potential melastatin 2 (TRPM2) in pancreatic cancer cells (51). TRPM2, a nonspecific Ca^{2+} channel, has been shown to mediate glucose- and incretin-induced insulin secretion (52–55). As SIRT6-deficient β cells exhibit mitochondrial defects and insufficient ATP production (23), it is likely that the indirect effect of SIRT6 deficiency on Ca^{2+} flux also plays a significant role. In this study, we observed a connection from SIRT6 to REM2, a potent endogenous inhibitor of high-voltage-activated Ca^{2+} channels. The *REM2* gene is negatively regulated in β cells by SIRT6 in a catalytic activity-dependent manner. Significantly, knockdown of *REM2* partially rescues SIRT6-deficiency- and palmitic acids-induced DNA damage and multiple forms of cell death. Additionally, β-cell-specific *Rem2* gene knockout in mice leads to a significant increase in β cell mass and a decrease in β cell apoptosis and improved glucose tolerance. The role of REM2 in β cells seems much different from that in embryonic stem cells and embryos. Previously, it has been reported that REM2 maintains hESCs by suppressing the p53 transcriptional activity and cyclin D1 expression and localization (32). Knockdown of *Rem2* in zebrafish embryos leads to loss of neural tissue due to increased apoptosis and decreased proliferation at 36 hours of early development (31). Interestingly, SIRT6 also negatively regulates p53 by deacetylating lysine 381 of p53 protein. p53 haploinsufficiency significantly extends the lifespan of SIRT6-deficient mice partly by reducing senescence and apoptosis (56). In addition to Ca^{2+} channels, REM2 has been shown to inhibit CaMKII in neurons (28). As CamKII positively regulates insulin secretion in pancreatic β cells (57–59), it is plausible that SIRT6 also regulates insulin secretion through suppression of the *REM2* gene expression and an indirect activation of Ca^{2+} channels and CamKII.

In summary, our data suggest that SIRT6 is an important factor that helps maintain pancreatic β cell survival and function during aging. Age-associated SIRT6 insufficiency in β cells increases the risk of DNA damage and cell death. Therefore, improving SIRT6 function may ameliorate pathological changes such as glucose intolerance or diabetes associated with unhealthy aging β cells.

Supplementary Material

Refer to Web version on PubMed Central for supplementary material.

Funding:

This work was supported in part by the National Institute of Diabetes and Digestive and Kidney Diseases (R01DK121925, R01DK120689, and R01DK124612, P30DK097512) and the National Institute on Aging (R21AG072288).

Data availability:

RNA-seq data (GSE287696) has been deposited to the GEO database and it will be available on August 23, 2025.

Abbreviations:

AUC	area under the curve
CaMKII	calcium/calmodulin dependent kinase II
GSIS	glucose-stimulated insulin secretion
GTT	glucose tolerance test
hESC	human embryonic stem cell
HVACC	high-voltage-activated calcium channel
PA	Palmitic Acid
REM2	RRAD and Gem like GTPase 2
SIRT6	Sirtuin 6
TUNEL	terminal deoxynucleotidyl transferase dUTP nick end labeling

References

1. De Tata V Age-related impairment of pancreatic Beta-cell function: pathophysiological and cellular mechanisms. Front Endocrinol (Lausanne) 2014;5:138. [PubMed: 25232350]
2. Szoke E, Shrayyef MZ, Messing S, Woerle HJ, van Haeften TW, Meyer C, Mitrakou A, et al. Effect of aging on glucose homeostasis: accelerated deterioration of beta-cell function in individuals with impaired glucose tolerance. Diabetes Care 2008;31:539–543. [PubMed: 18083793]
3. Tuduri E, Soriano S, Almagro L, Montanya E, Alonso-Magdalena P, Nadal A, Quesada I. The pancreatic beta-cell in ageing: Implications in age-related diabetes. Ageing Res Rev 2022;80:101674. [PubMed: 35724861]
4. Aguayo-Mazzucato C. Functional changes in beta cells during ageing and senescence. Diabetologia 2020;63:2022–2029. [PubMed: 32894312]
5. Li L, Trifunovic A, Kohler M, Wang Y, Petrovic Berglund J, Illies C, Juntti-Berggren L, et al. Defects in beta-cell Ca2+ dynamics in age-induced diabetes. Diabetes 2014;63:4100–4114. [PubMed: 24985350]
6. Westacott MJ, Farnsworth NL, St Clair JR, Poffenberger G, Heintz A, Ludin NW, Hart NJ, et al. Age-Dependent Decline in the Coordinated [Ca2+] and Insulin Secretory Dynamics in Human Pancreatic Islets. Diabetes 2017;66:2436–2445. [PubMed: 28588099]
7. Barlow J, Jensen VH, Jastroch M, Affourtit C. Palmitate-induced impairment of glucose-stimulated insulin secretion precedes mitochondrial dysfunction in mouse pancreatic islets. Biochem J 2016;473:487–496. [PubMed: 26621874]
8. Basu R, Breda E, Oberg AL, Powell CC, Dalla Man C, Basu A, Vittone JL, et al. Mechanisms of the age-associated deterioration in glucose tolerance: contribution of alterations in insulin secretion, action, and clearance. Diabetes 2003;52:1738–1748. [PubMed: 12829641]
9. Fontes G, Zarrouki B, Hagman DK, Latour MG, Semache M, Roskens V, Moore PC, et al. Glucolipotoxicity age-dependently impairs beta cell function in rats despite a marked increase in beta cell mass. Diabetologia 2010;53:2369–2379. [PubMed: 20628728]

10. Xiong X, Sun X, Wang Q, Qian X, Zhang Y, Pan X, Dong XC. SIRT6 protects against palmitate-induced pancreatic beta-cell dysfunction and apoptosis. J Endocrinol 2016;231:159–165. [PubMed: 27601447]
11. Mostoslavsky R, Chua KF, Lombard DB, Pang WW, Fischer MR, Gellon L, Liu P, et al. Genomic instability and aging-like phenotype in the absence of mammalian SIRT6. Cell 2006;124:315–329. [PubMed: 16439206]
12. Kanfi Y, Naiman S, Amir G, Peshti V, Zinman G, Nahum L, Bar-Joseph Z, et al. The sirtuin SIRT6 regulates lifespan in male mice. Nature 2012;483:218–221. [PubMed: 22367546]
13. Zhang W, Wan H, Feng G, Qu J, Wang J, Jing Y, Ren R, et al. SIRT6 deficiency results in developmental retardation in cynomolgus monkeys. Nature 2018;560:661–665. [PubMed: 30135584]
14. Dong XC. Sirtuin 6-A Key Regulator of Hepatic Lipid Metabolism and Liver Health. Cells 2023;12.
15. Korotkov A, Seluanov A, Gorbunova V. Sirtuin 6: linking longevity with genome and epigenome stability. Trends Cell Biol 2021.
16. Kugel S, Mostoslavsky R. Chromatin and beyond: the multitasking roles for SIRT6. Trends Biochem Sci 2014;39:72–81. [PubMed: 24438746]
17. Roichman A, Elhanati S, Aon MA, Abramovich I, Di Francesco A, Shahar Y, Avivi MY, et al. Restoration of energy homeostasis by SIRT6 extends healthy lifespan. Nat Commun 2021;12:3208. [PubMed: 34050173]
18. Toiber D, Erdel F, Bouazoune K, Silberman DM, Zhong L, Mulligan P, Sebastian C, et al. SIRT6 recruits SNF2H to DNA break sites, preventing genomic instability through chromatin remodeling. Mol Cell 2013;51:454–468. [PubMed: 23911928]
19. Zhong L, D'Urso A, Toiber D, Sebastian C, Henry RE, Vadysirisack DD, Guimaraes A, et al. The histone deacetylase Sirt6 regulates glucose homeostasis via Hif1alpha. Cell 2010;140:280–293. [PubMed: 20141841]
20. Zhong X, Huang M, Kim HG, Zhang Y, Chowdhury K, Cai W, Saxena R, et al. SIRT6 Protects Against Liver Fibrosis by Deacetylation and Suppression of SMAD3 in Hepatic Stellate Cells. Cell Mol Gastroenterol Hepatol 2020;10:341–364. [PubMed: 32305562]
21. Kanfi Y, Peshti V, Gil R, Naiman S, Nahum L, Levin E, Kronfeld-Schor N, et al. SIRT6 protects against pathological damage caused by diet-induced obesity. Aging Cell 2010;9:162–173. [PubMed: 20047575]
22. Qin K, Zhang N, Zhang Z, Nipper M, Zhu Z, Leighton J, Xu K, et al. SIRT6-mediated transcriptional suppression of Txnip is critical for pancreatic beta cell function and survival in mice. Diabetologia 2018;61:906–918. [PubMed: 29322219]
23. Xiong X, Wang G, Tao R, Wu P, Kono T, Li K, Ding WX, et al. Sirtuin 6 regulates glucose-stimulated insulin secretion in mouse pancreatic beta cells. Diabetologia 2016;59:151–160. [PubMed: 26471901]
24. Song MY, Wang J, Ka SO, Bae EJ, Park BH. Insulin secretion impairment in Sirt6 knockout pancreatic beta cells is mediated by suppression of the FoxO1-Pdx1-Glut2 pathway. Sci Rep 2016;6:30321. [PubMed: 27457971]
25. Yang T, Colecraft HM. Regulation of voltage-dependent calcium channels by RGK proteins. Biochim Biophys Acta 2013;1828:1644–1654. [PubMed: 23063948]
26. Finlin BS, Mosley AL, Crump SM, Correll RN, Ozcan S, Satin J, Andres DA. Regulation of L-type Ca2+ channel activity and insulin secretion by the Rem2 GTPase. J Biol Chem 2005;280:41864–41871. [PubMed: 15728182]
27. Yang T, Puckerin A, Colecraft HM. Distinct RGK GTPases differentially use alpha1- and auxiliary beta-binding-dependent mechanisms to inhibit CaV1.2/CaV2.2 channels. PLoS One 2012;7:e37079. [PubMed: 22590648]
28. Royer L, Herzog JJ, Kenny K, Tzvetkova B, Cochrane JC, Marr MT 2nd, Paradis S. The Ras-like GTPase Rem2 is a potent inhibitor of calcium/calmodulin-dependent kinase II activity. J Biol Chem 2018;293:14798–14811. [PubMed: 30072381]

29. Chai S, Wan X, Ramirez-Navarro A, Tesar PJ, Kaufman ES, Ficker E, George AL Jr., et al. Physiological genomics identifies genetic modifiers of long QT syndrome type 2 severity. J Clin Invest 2018;128:1043–1056. [PubMed: 29431731]
30. Liput DJ, Lu VB, Davis MI, Puhl HL, Ikeda SR. Rem2, a member of the RGK family of small GTPases, is enriched in nuclei of the basal ganglia. Sci Rep 2016;6:25137. [PubMed: 27118437]
31. Edel MJ, Boue S, Menchon C, Sanchez-Danes A, Izpisua Belmonte JC. Rem2 GTPase controls proliferation and apoptosis of neurons during embryo development. Cell Cycle 2010;9:3414–3422. [PubMed: 20729629]
32. Edel MJ, Menchon C, Menendez S, Consiglio A, Raya A, Izpisua Belmonte JC. Rem2 GTPase maintains survival of human embryonic stem cells as well as enhancing reprogramming by regulating p53 and cyclin D1. Genes Dev 2010;24:561–573. [PubMed: 20231315]
33. Bierings R, Beato M, Edel MJ. An endothelial cell genetic screen identifies the GTPase Rem2 as a suppressor of p19ARF expression that promotes endothelial cell proliferation and angiogenesis. J Biol Chem 2008;283:4408–4416. [PubMed: 18056257]
34. Kim HG, Huang M, Xin Y, Zhang Y, Zhang X, Wang G, Liu S, et al. The epigenetic regulator SIRT6 protects the liver from alcohol-induced tissue injury by reducing oxidative stress in mice. J Hepatol 2019;71:960–969. [PubMed: 31295533]
35. Stull ND, Breite A, McCarthy R, Tersey SA, Mirmira RG. Mouse islet of Langerhans isolation using a combination of purified collagenase and neutral protease. J Vis Exp 2012.
36. Hohmeier HE, Mulder H, Chen G, Henkel-Rieger R, Prentki M, Newgard CB. Isolation of INS-1-derived cell lines with robust ATP-sensitive K+ channel-dependent and -independent glucose-stimulated insulin secretion. Diabetes 2000;49:424–430. [PubMed: 10868964]
37. Rao X, Huang X, Zhou Z, Lin X. An improvement of the 2^(-delta delta CT) method for quantitative real-time polymerase chain reaction data analysis. Biostat Bioinforma Biomath 2013;3:71–85. [PubMed: 25558171]
38. Xiao C, Kim HS, Lahusen T, Wang RH, Xu X, Gavrilova O, Jou W, et al. SIRT6 deficiency results in severe hypoglycemia by enhancing both basal and insulin-stimulated glucose uptake in mice. J Biol Chem 2010;285:36776–36784. [PubMed: 20847051]
39. Mao Z, Hine C, Tian X, Van Meter M, Au M, Vaidya A, Seluanov A, et al. SIRT6 promotes DNA repair under stress by activating PARP1. Science 2011;332:1443–1446. [PubMed: 21680843]
40. Tian X, Firsanov D, Zhang Z, Cheng Y, Luo L, Tombline G, Tan R, et al. SIRT6 Is Responsible for More Efficient DNA Double-Strand Break Repair in Long-Lived Species. Cell 2019;177:622–638 e622. [PubMed: 31002797]
41. Bandopadhyay S, Prasad P, Ray U, Das Ghosh D, Roy SS. SIRT6 promotes mitochondrial fission and subsequent cellular invasion in ovarian cancer. FEBS Open Bio 2022;12:1657–1676.
42. Zhou Y, Fan X, Jiao T, Li W, Chen P, Jiang Y, Sun J, et al. SIRT6 as a key event linking P53 and NRF2 counteracts APAP-induced hepatotoxicity through inhibiting oxidative stress and promoting hepatocyte proliferation. Acta Pharm Sin B 2021;11:89–99. [PubMed: 33532182]
43. Grootaert MOJ, Finigan A, Figg NL, Uryga AK, Bennett MR. SIRT6 Protects Smooth Muscle Cells From Senescence and Reduces Atherosclerosis. Circ Res 2021;128:474–491. [PubMed: 33353368]
44. Lee OH, Woo YM, Moon S, Lee J, Park H, Jang H, Park YY, et al. Sirtuin 6 deficiency induces endothelial cell senescence via downregulation of forkhead box M1 expression. Aging (Albany NY) 2020;12:20946–20967. [PubMed: 33171439]
45. Han LL, Jia L, Wu F, Huang C. Sirtuin6 (SIRT6) Promotes the EMT of Hepatocellular Carcinoma by Stimulating Autophagic Degradation of E-Cadherin. Mol Cancer Res 2019;17:2267–2280. [PubMed: 31551254]
46. Zhang S, Jiang S, Wang H, Di W, Deng C, Jin Z, Yi W, et al. SIRT6 protects against hepatic ischemia/reperfusion injury by inhibiting apoptosis and autophagy related cell death. Free Radic Biol Med 2018;115:18–30. [PubMed: 29129519]
47. Fu W, Li H, Fu H, Zhao S, Shi W, Sun M, Li Y. The SIRT3 and SIRT6 Promote Prostate Cancer Progression by Inhibiting Necroptosis-Mediated Innate Immune Response. J Immunol Res 2020;2020:8820355. [PubMed: 33282964]

48. Huang J, Dong S, Wu Y, Yi H, Zhang W, Ai X. Sirtuin 6 Deacetylates Apoptosis-Associated Speck-Like Protein (ASC) to Inhibit Endothelial Cell Pyroptosis in Atherosclerosis. Int Heart J 2024;65:466–474. [PubMed: 38749754]

49. Yao F, Lv X, Jin Z, Chen D, Zheng Z, Yang J, Ren L, et al. Sirt6 inhibits vascular endothelial cell pyroptosis by regulation of the Lin28b/let-7 pathway in atherosclerosis. Int Immunopharmacol 2022;110:109056. [PubMed: 35978508]

50. Barker CJ, Li L, Kohler M, Berggren PO. beta-Cell Ca(2+) dynamics and function are compromised in aging. Adv Biol Regul 2015;57:112–119. [PubMed: 25282681]

51. Bauer I, Grozio A, Lasiglie D, Basile G, Sturla L, Magnone M, Sociali G, et al. The NAD+-dependent histone deacetylase SIRT6 promotes cytokine production and migration in pancreatic cancer cells by regulating Ca2+ responses. J Biol Chem 2012;287:40924–40937. [PubMed: 23086953]

52. Uchida K, Dezaki K, Damdindorj B, Inada H, Shiuchi T, Mori Y, Yada T, et al. Lack of TRPM2 impaired insulin secretion and glucose metabolisms in mice. Diabetes 2011;60:119–126. [PubMed: 20921208]

53. Pang B, Kim S, Li D, Ma Z, Sun B, Zhang X, Wu Z, et al. Glucagon-like peptide-1 potentiates glucose-stimulated insulin secretion via the transient receptor potential melastatin 2 channel. Exp Ther Med 2017;14:5219–5227. [PubMed: 29201240]

54. Kashio M, Tominaga M. Redox Signal-mediated Enhancement of the Temperature Sensitivity of Transient Receptor Potential Melastatin 2 (TRPM2) Elevates Glucose-induced Insulin Secretion from Pancreatic Islets. J Biol Chem 2015;290:12435–12442. [PubMed: 25817999]

55. Yosida M, Dezaki K, Uchida K, Kodera S, Lam NV, Ito K, Rita RS, et al. Involvement of cAMP/EPAC/TRPM2 activation in glucose- and incretin-induced insulin secretion. Diabetes 2014;63:3394–3403. [PubMed: 24824430]

56. Ghosh S, Wong SK, Jiang Z, Liu B, Wang Y, Hao Q, Gorbunova V, et al. Haploinsufficiency of Trp53 dramatically extends the lifespan of Sirt6-deficient mice. Elife 2018;7.

57. Dixit SS, Wang T, Manzano EJ, Yoo S, Lee J, Chiang DY, Ryan N, et al. Effects of CaMKII-mediated phosphorylation of ryanodine receptor type 2 on islet calcium handling, insulin secretion, and glucose tolerance. PLoS One 2013;8:e58655. [PubMed: 23516528]

58. Dadi PK, Vierra NC, Ustione A, Piston DW, Colbran RJ, Jacobson DA. Inhibition of pancreatic beta-cell Ca2+/calmodulin-dependent protein kinase II reduces glucose-stimulated calcium influx and insulin secretion, impairing glucose tolerance. J Biol Chem 2014;289:12435–12445. [PubMed: 24627477]

59. Santos GJ, Ferreira SM, Ortis F, Rezende LF, Li C, Naji A, Carneiro EM, et al. Metabolic memory of ss-cells controls insulin secretion and is mediated by CaMKII. Mol Metab 2014;3:484–489. [PubMed: 24944908]

Highlights

- Pancreatic β-cell function declines with age, but the underlying mechanism is poorly understood.
- In this study, we attempted to address how to reverse β-cell aging
- Our data showed that SIRT6 overexpression can reduce age-associated DNA damage, cell death, and functional decline in β cells.
- Our findings suggest that improving SIRT6 gene expression/function may slow down β-cell decline in old patients.

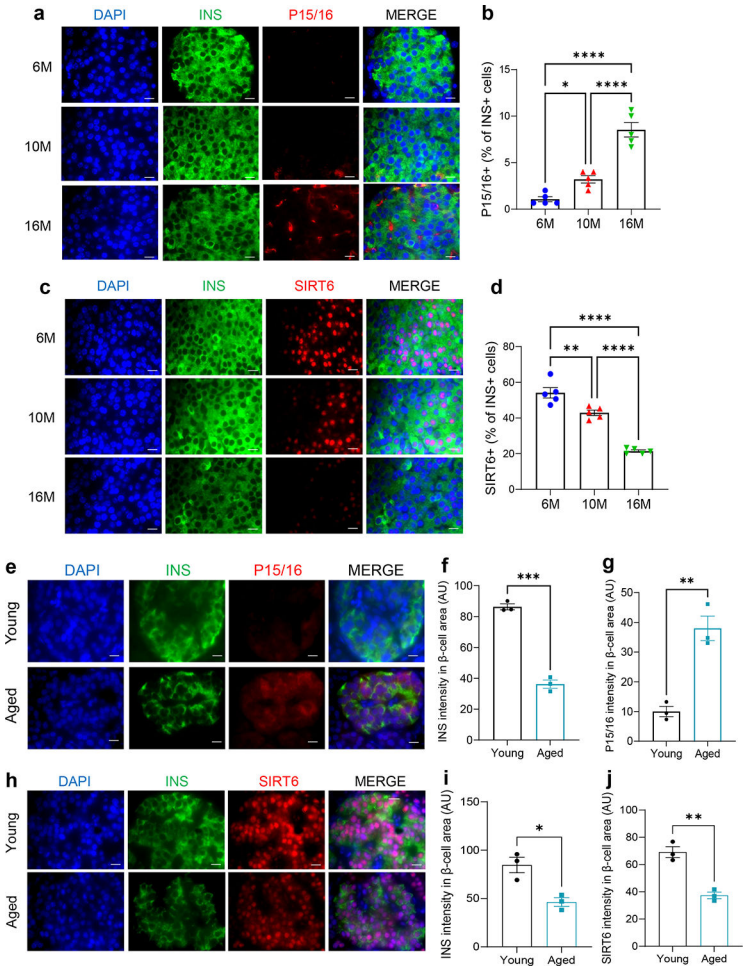

Figure 1. SIRT6 is decreased and senescence is increased in aged β cells.

(**a, b**) Immunofluorescent staining and quantification of insulin (INS) and P15/16 in pancreatic sections from male mice at 6, 10, and 16 months of age (n=5). (**c, d**) Immunofluorescent staining and quantification of INS and SIRT6 staining in pancreatic sections from male mice at 6, 10, and 16 months of age (*n*=5). (**e-g**) Immunofluorescent staining and quantification of INS and P15/16 in young and aged human pancreatic sections (n=3). (**h-j**) Immunofluorescent staining and quantification of INS and SIRT6 in young and aged human pancreatic sections (n=3). Scale bar = 15 μm. Data are presented as mean ±SEM. *P<0.05, **P<0.01, and ****P<0.0001.

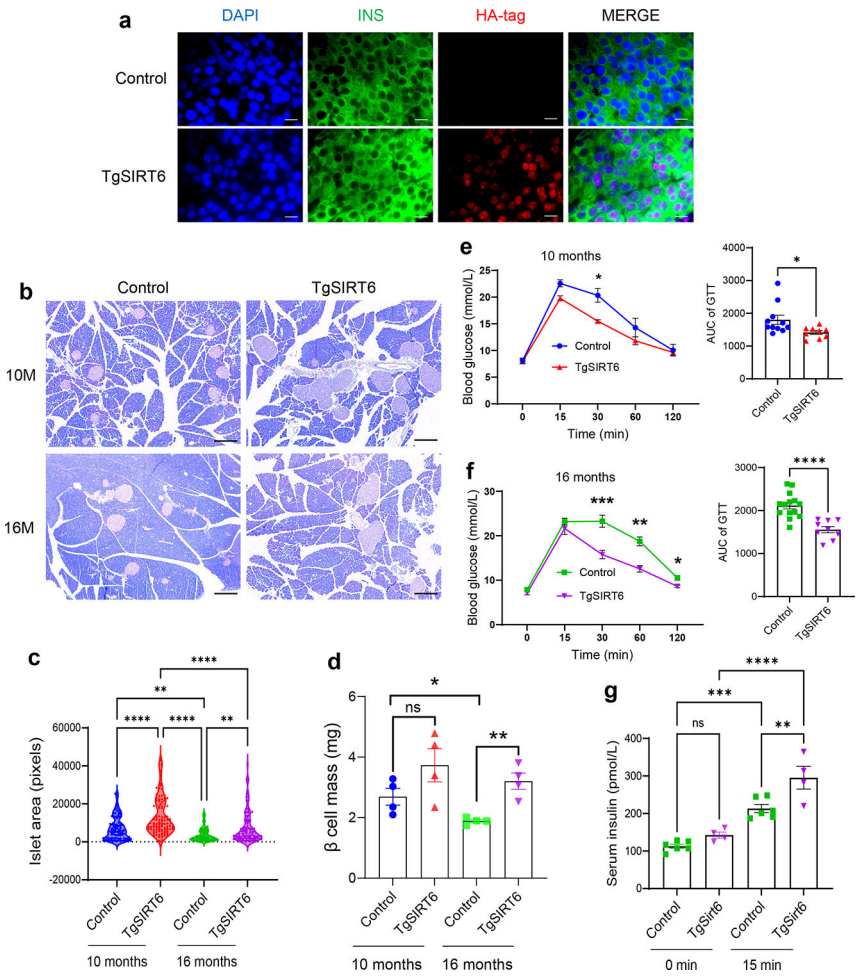

Figure 2. Pancreatic β-cell-specific SIRT6 overexpression improves β-cell mass, insulin secretion, and glucose tolerance in mice during aging.

(**a**) Validation of SIRT6 transgene (with an HA tag) expression by immunofluorescent staining of pancreatic sections. Scale bar = 15 μm. (**b**) Representative histological images of pancreatic sections from control and TgSIRT6 male mice at 10 and 16 months of age (n=4–6). Scale bar = 400 μm. (**c**) Quantification of pancreatic islet areas in control and TgSIRT6 male mice at 10 and 16 months of age. (**d**) β-cell mass analysis in control and TgSIRT6 male and female mice (n=4) at 10 and 16 months of age. (**e, f**) Glucose tolerance tests were performed in control and TgSIRT6 male mice at 10 and 16 months of age (n=9–14). Blood glucose levels are shown as a function of time (left panels) and area under the curve (AUC) values are shown on the right. (**g**) Glucose-stimulated insulin secretion was performed in 16-month-old male mice (n=4–6). Serum insulin levels were measured at baseline and 15 minutes after injection of a bolus of glucose. Data are represented as mean ± SEM. *$p <$ 0.05, **$p < 0.01$, ***$p < 0.001$, ****$p < 0.0001$.

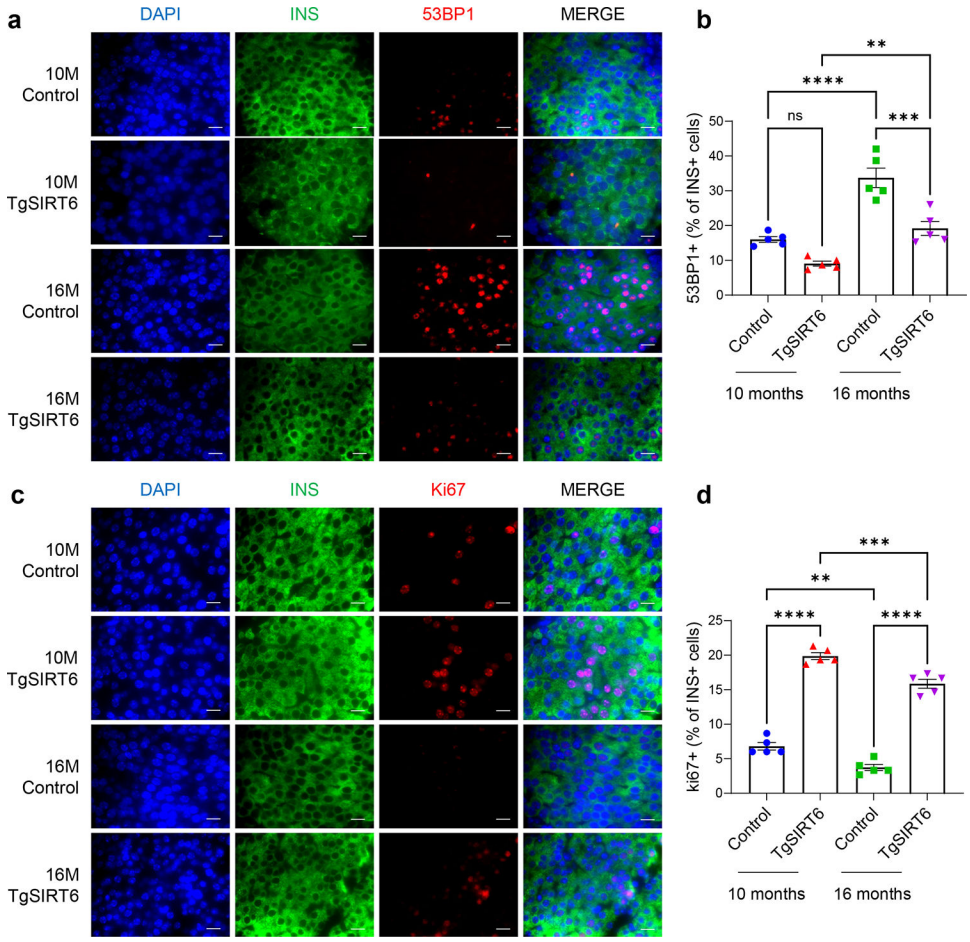

Figure 3. SIRT6 overexpression in pancreatic β cells reduces DNA damage and increases cell proliferation.

(**a**) Immunofluorescent staining of INS (green) and 53BP1 (red) in pancreatic sections from control and TgSIRT6 male mice at 10 and 16 months of age (n=5). (**b**) Quantification of the percentages of 53BP1$^+$ β cells in panel a. (**c**) Immunofluorescent staining of INS (green) and Ki67 (red) in pancreatic sections from control and TgSIRT6 male mice at 10 and 16 months of age (n=5). (**d**) Quantification of the percentages of Ki67$^+$ β cells in panel c. Scale bar = 15 μm. Data are presented as mean ±SEM. *p<0.05, **p<0.01, ***p<0.001 ****p<0.0001.

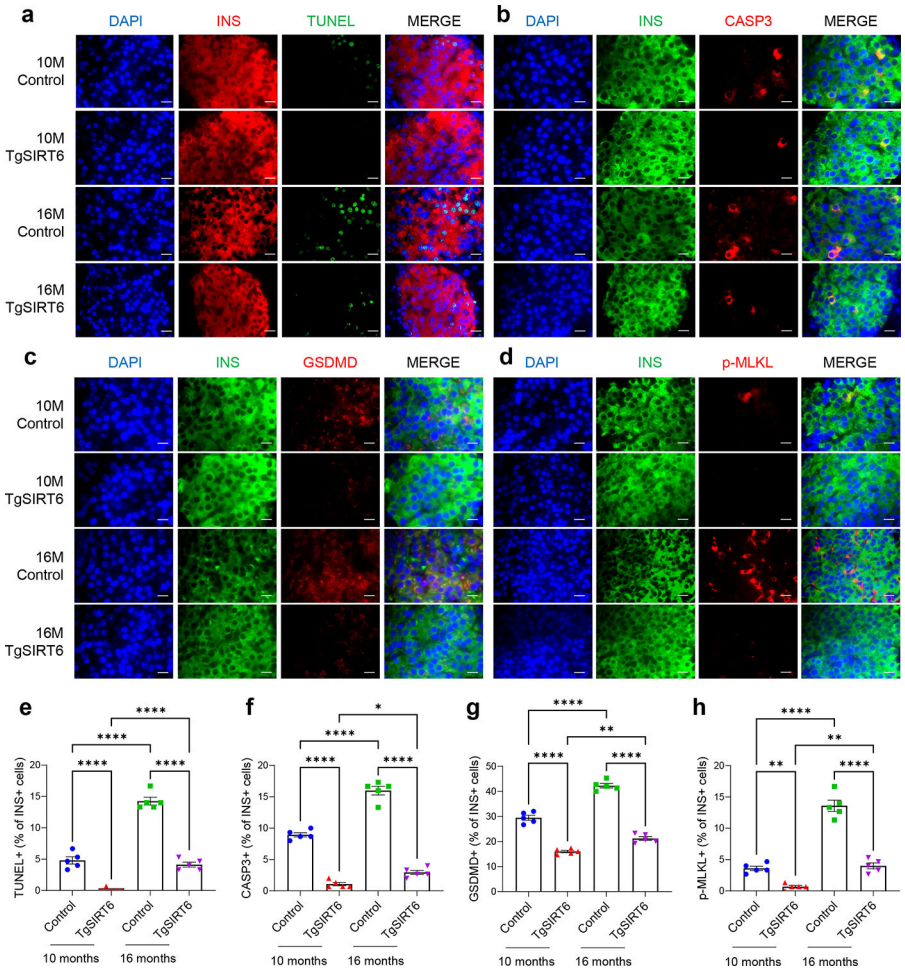

Figure 4. SIRT6 overexpression reduces apoptosis, necroptosis, and pyroptosis in mouse pancreatic β cells during aging.

(**a**) Immunofluorescent staining of INS (red) and TUNEL (green) in pancreatic sections from control and TgSIRT6 male mice at 10 and 16 months of age (n=5). (**b**) Immunofluorescent staining of INS (green) and cleaved CASP3 (red), an apoptosis marker, in male mouse pancreatic sections (n=5). (**c**) Immunofluorescent staining of INS (green) and GSDMD (red), a pyroptosis marker, in male mouse pancreatic sections (n=5). (**d**) Immunofluorescent staining of INS (green) and phospho-MLKL (p-MLKL, red), a necroptosis marker, in male mouse pancreatic sections (n=5). (**e-h**) Quantification of TUNEL$^+$, CASP3$^+$, GSDMD$^+$, and p-MLKL$^+$ β cells in control and TgSIRT6 mouse pancreatic sections, respectively. Scale bar = 15 μm. Data are presented as mean ±SEM *p<0.05, **p<0.01, ***p<0.001 ****p<0.0001.

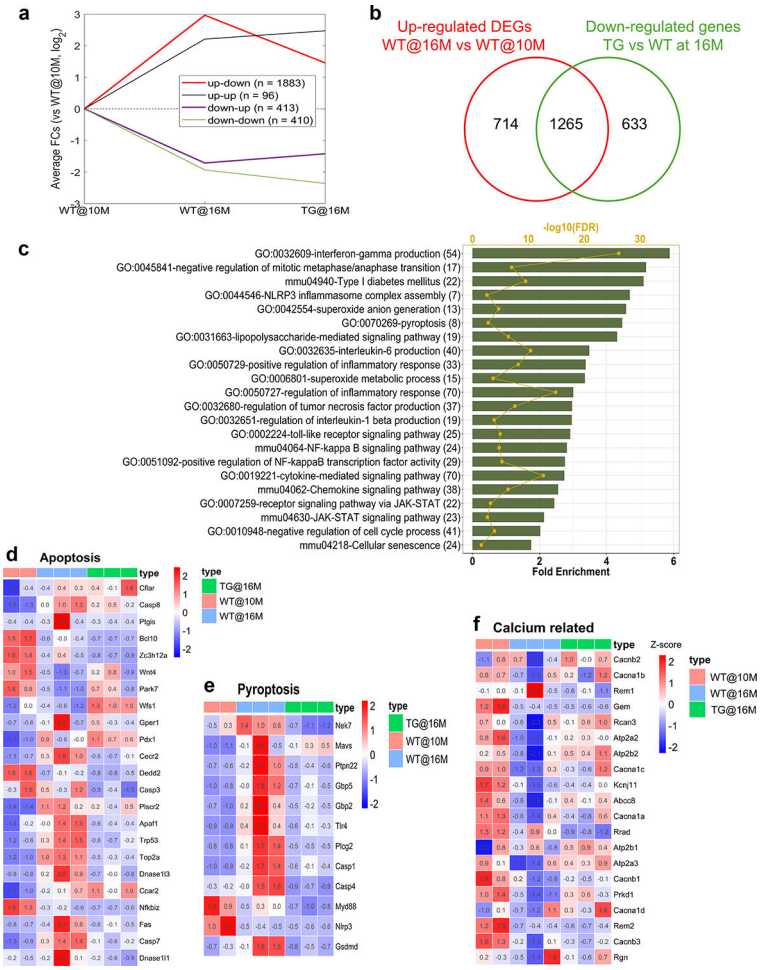

Figure 5. Transcriptomic analysis of differential genes and pathways in control and TgSIRT6 mouse islets.

(**a**) Transcriptomic shifts in mouse islets by age and genotype from 10 to 16 months of age. (**b**) Venn diagram representation of shared genes between upregulated DEGs in 16-month WT (n=3) vs. 10-month WT (n=2) mouse islets and downregulated DEGs in 16-month TG (n=3) vs. 16-month WT (n=3) mouse islets. (**c**) Representative biological processes in the common DEGs in panel b. (**d-f**) Heatmap illustrations of expression of genes in apoptosis, pyroptosis, and calcium regulation in 10-month WT, 16-month WT, and 16-month TgSIRT6 mouse islets (n=2–3).

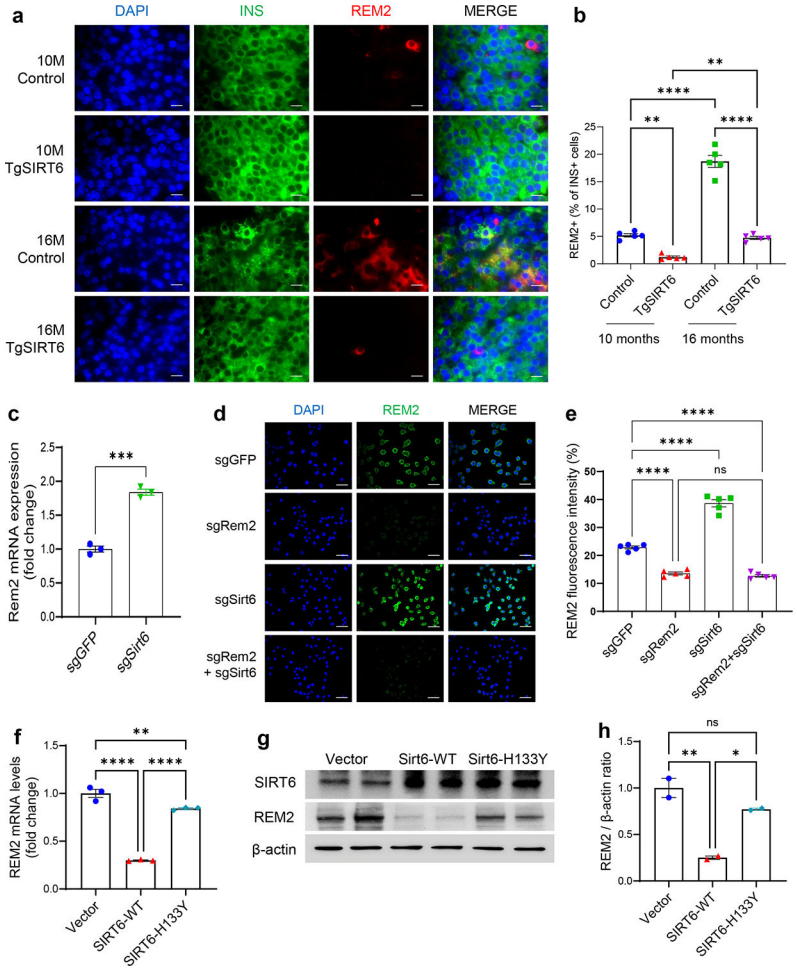

Figure 6. SIRT6 negatively impacts the *Rem2* gene expression in pancreatic β cells.

(a) Immunofluorescent staining of INS and REM2 in pancreatic sections from 10 and 16 months old control and TgSIRT6 male mice (n=5). Scale bar = 15 μm. (**b**) Quantification of percentages of $REM2^+$ INS^+ β cells in both control and TgSIRT6 mice in Panel a. **(c)** Rem2 mRNA analysis in INS-1 cells transfected with either control sgGFP or sgSirt6 (n=3). **(d)** Immunofluorescent staining of REM2 in INS-1 cells transfected with sgGFP, sgRem2, sgSirt6, or both. Scale bar = 50 μm. (**e**) Quantification of REM2 fluorescence intensity in Panel d. (**f**) REM2 mRNA levels in INS-1 cells transfected with vector control, WT SIRT6, or SIRT6-H133Y mutant (a SIRT6 catalytically inactive mutant) plasmids (n=3). (**g**) Western blot analysis of REM2 protein levels in INS-1 cells transfected with vector control, WT SIRT6, or SIRT6-H133Y mutant plasmids. β-actin serves as a loading control. **(h)** Quantification of REM2 protein levels in panel g. Data are presented as mean ±SEM. *p<0.05, **p<0.01, ***p<0.001 ****p<0.0001.

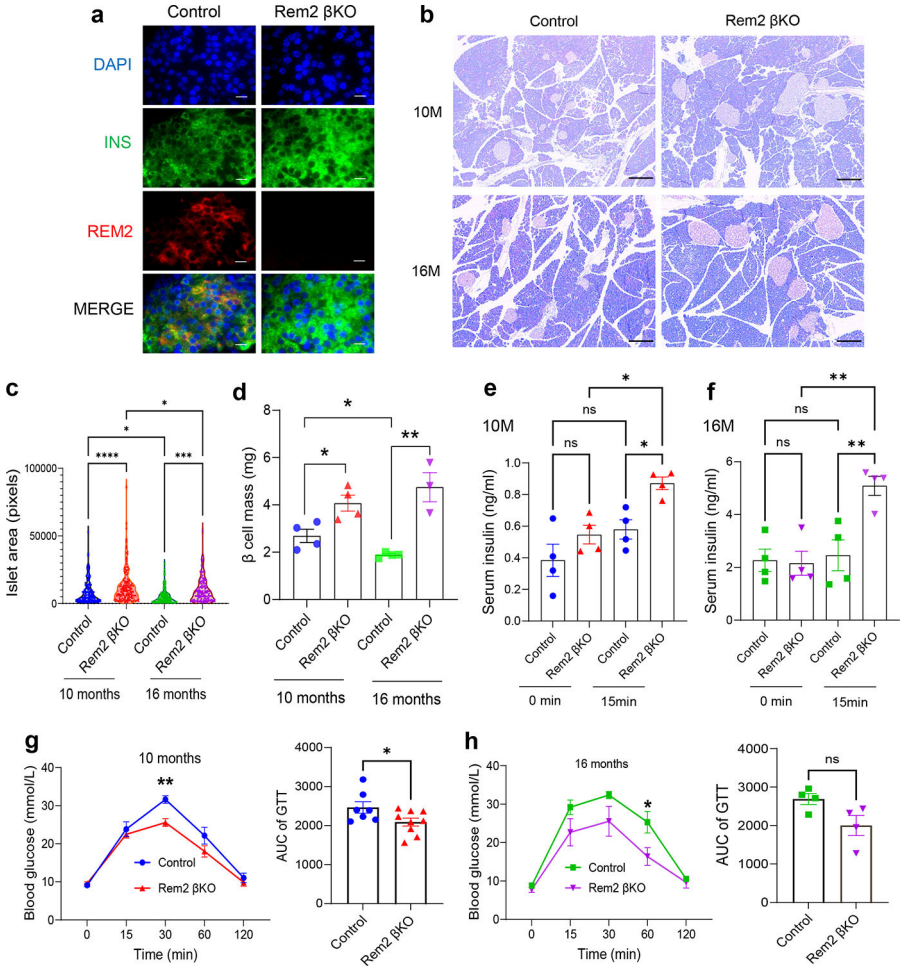

Figure 7. *Rem2* β-cell-specific knockout improves β-cell mass and glucose tolerance.

(**a**) Confirmation of β-cell-specific Rem2 knockout in male and female mice at 10 months of age by immunostaining analysis. Scale bar = 15 μm. (**b**) Representative histological images of pancreatic sections from 10- and 16-month-old control and *Rem2* β-cell-specific KO male mice (n=5). Scale bar = 400 μm. (**c**) Quantification of pancreatic islet areas in control and *Rem2* βKO mice. (**d**) β-cell mass analysis in control and *Rem2* βKO mice (n=4). (**e, f**) Glucose-stimulated insulin secretion in 10- and 16-month control and *Rem2* βKO mice (n=4). (**g**) Glucose tolerance tests and area under the curve analysis in 10-month control (n=7) and *Rem2* βKO (n=9) mice. (**h**) Glucose tolerance tests and area under the curve analysis in 16-month control and *Rem2* βKO (n=4) mice. Data are presented as mean ±SEM. *p<0.05, **p<0.01, ***p<0.001 ****p<0.0001.

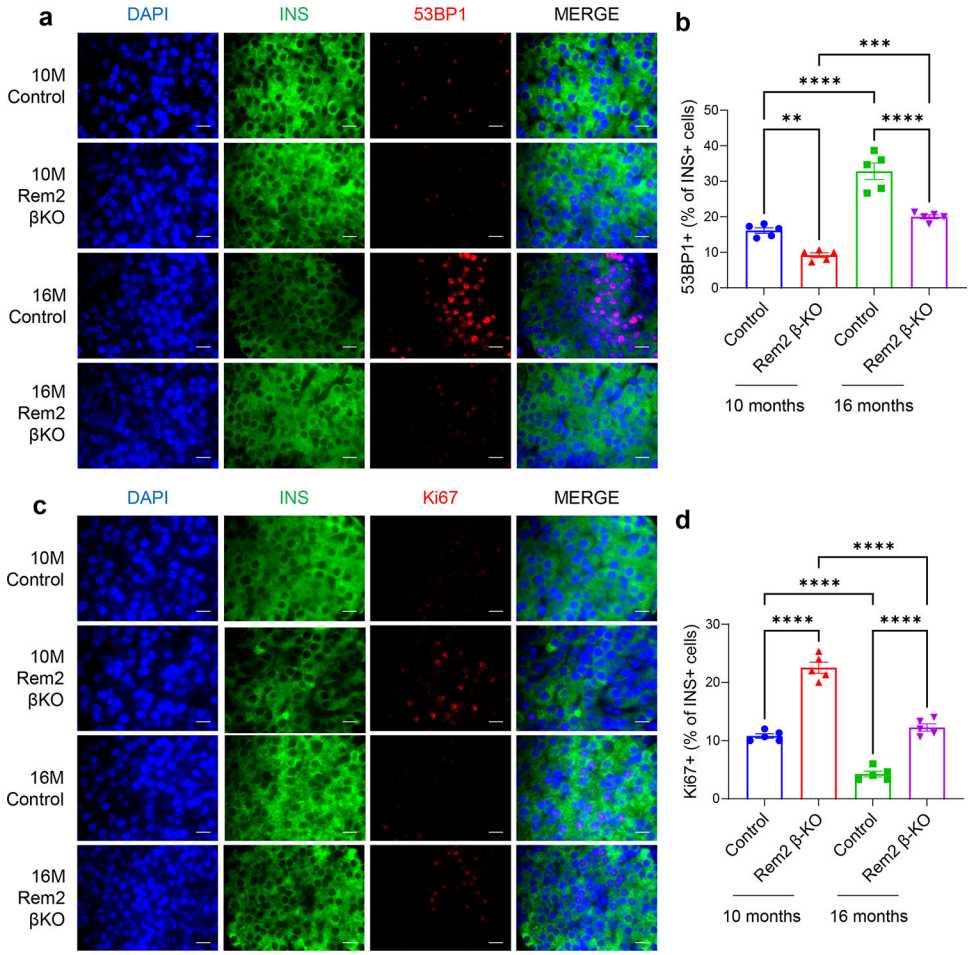

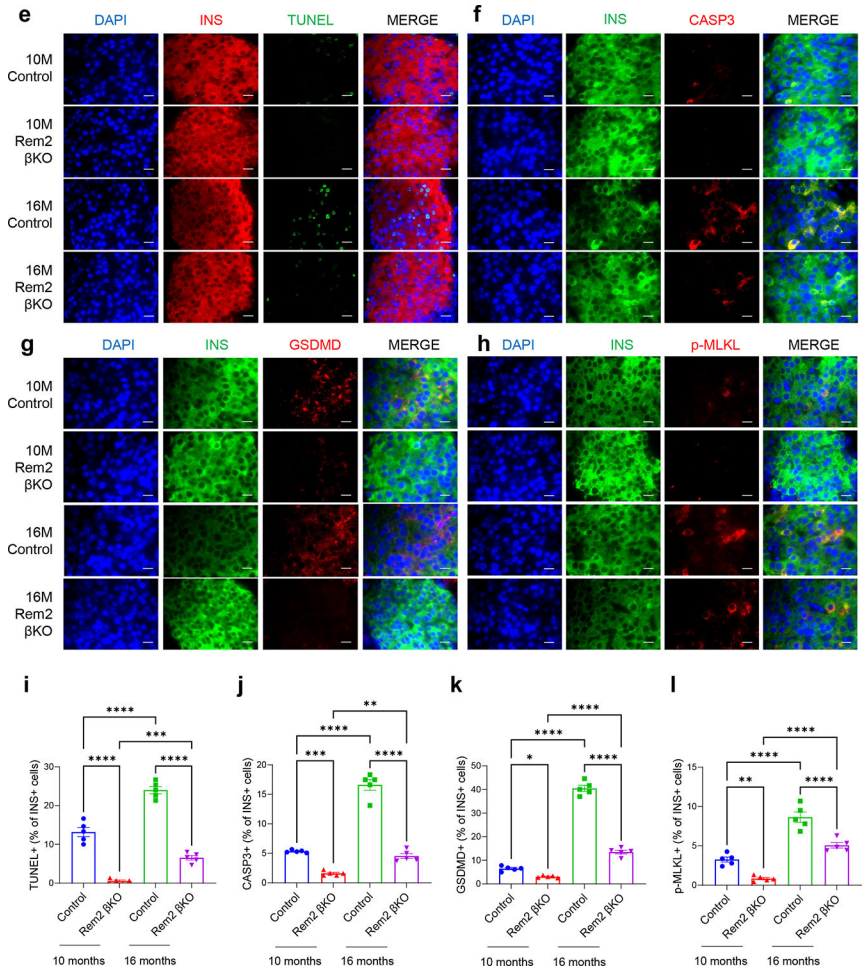

Fig. 8. Deletion of Rem2 in pancreatic β cells reduces age-associated DNA damage and cell death.

(a, b) Immunofluorescence and quantification analysis of 53BP1 in pancreatic sections from control and *Rem2* βKO male and female mice (n=5). **(c, d)** Immunofluorescence and quantification analysis of Ki67 in control and *Rem2* βKO male and female mouse pancreatic sections. **(e)** TUNEL assays in control and *Rem2* βKO male and female mouse pancreatic sections (n=5). **(f)** Cleaved CASP3 staining in control and *Rem2* βKO male and female mouse pancreatic sections (n=5). **(g)** GSDMD staining in control and *Rem2* βKO male and female mouse pancreatic sections (n=5). **(h)** p-MLKL staining in control and *Rem2* βKO male and female mouse pancreatic sections (n=5). **(i-l)** Quantification of TUNEL$^+$, CASP3$^+$, GSDMD$^+$, and p-MLKL$^+$ β cells in control and *Rem2* βKO mouse pancreatic sections in panels e-h. Scale bar = 15 μm. Data are represented as mean ± SEM. **p< 0.01, ***p< 0.001, ****p< 0.0001.